PAPR Reduction for Hybrid ACO-OFDM Aided IM/DD Optical Wireless Vehicular Communications

Baolong Li, Wei Xu, *Senior Member, IEEE*, Hua Zhang, *Member, IEEE*, Chunming Zhao, *Member, IEEE*, and Lajos Hanzo, *Fellow, IEEE*

***Abstract*—Hybrid asymmetrically clipped optical orthogonal frequency division multiplexing (HACO-OFDM) improves the spectral efficiency compared to asymmetrically clipped optical OFDM (ACO-OFDM) and pulse-amplitude-modulated discrete multitone (PAM-DMT) modulation, while retaining the advantage of high power efficiency. HACO-OFDM has found favor in numerous applications, but its peak-to-average-power ratio (PAPR) has remained a concern in optical wireless communications, since the family of existing PAPR reduction methods cannot be directly invoked for the superimposed HACO-OFDM signals. Hence, we analyze the characteristics of HACO-OFDM signals and develop a specific PAPR reduction technique relying on tone injection. Our numerical results show that the proposed method achieves significantly improved PAPR statistics compared to the conventional methods, leading to a significant bit error ratio (BER) reduction.**

***Index Terms*—Hybrid asymmetrically clipped optical orthogonal frequency division multiplexing (HACO-OFDM), optical wireless communications (OWC), peak-to-average-power ratio (PAPR) reduction.**

I. Introduction

Optical wireless communication (OWC) has gained significant attention owing to its compelling license-free operations, high security, low electromagnetic interference, etc. Orthogonal frequency division multiplexing (OFDM), which is deemed to be an effective technique of high-speed data transmission has been widely employed in OWC to achieve gigabit transmission [1].

In intensity modulated direct detection (IM/DD) OWC, the transmit signals are restricted to be non-negative due to the specific nature of the optical modulator [2], [3]. In order to guarantee non-negativity of the signals, unipolar OFDM schemes have been proposed. One of the popular schemes is known as direct-current-offset optical OFDM (DCO-OFDM), which renders the bipolar signals non-negative by adding a direct current (DC) component [4]. However, the DC component leads to power inefficiency since it does not convey any information [5]. The family of more power-efficient schemes includes asymmetrically clipped optical OFDM (ACO-OFDM) and pulse-amplitude-modulated discrete multitone (PAM-DMT), both of which exploit the beneficial properties of the Fourier transform and clip the negative signal to produce positive time-domain signals without losing any information [6], [7]. As a cost, both ACO-OFDM and PAM-DMT impose a reduction in spectral efficiency, since only half of the subcarriers or signal dimensions are actively exploited. Recently, the hybrid ACO-OFDM (HACO-OFDM) concept amalgamating both the techniques of ACO-OFDM and PAM-DMT has been proposed for IM/DD OWC [8]. Compared to ACO-OFDM and PAM-DMT, HACO-OFDM improves the spectral efficiency without degrading the attainable power efficiency [8], [9].

Despite its superior features, OFDM suffers from the inherent disadvantage of high peak-to-average power ratio (PAPR). In the context of OWC, the presence of high PAPR causes both in-band distortion and out-of-band radiation because of the non-linear characteristics of both the power amplifiers and of the light emitting diodes (LEDs) [10]. Unlike in radio frequency (RF) communications, the out-of-band radiation is much less of a problem in OFDM-based OWC due to the advantages of the license-free spectrum and inherent isolation of optical emissions [11], [12]. Additionally, since the optical LED transmitter also acts as a low pass filter, the out-of-band radiation can be suppressed in OWC systems [13]. However, the in-band distortion introduces non-linear distortion to the transmitted signals, which significantly deteriorates the achievable system performance [5], [14]. Therefore, PAPR reduction remains an essential issue in OFDM-based OWC systems [15]–[17].

Various PAPR reduction techniques conceived for OFDM-based OWC have been investigated, including clipping, null subcarrier shifting, tone injection, pilot-assisted methods and so on [15]–[20]. A recoverable upper-clipping procedure was proposed in [15] for ACO-OFDM to achieve a significant PAPR reduction. Chen *et al.* [16] proposed a novel null subcarrier shifting scheme for optical OFDM systems, which substantially mitigates the high PAPR of the OFDM signals. In [17], the method of tone injection optimization using semi-definite programming was applied in an DCO-OFDM system for PAPR reduction, and a reduction of 5 dB has been observed. In [18] and [19], a pilot-assisted PAPR reduction technique was advocated. A low-PAPR ACO-OFDM scheme was proposed in [20] for IM/DD systems, which has better non-linear distortion mitigation performance than the conventional scheme. However, in contrast to the typical optical OFDM (OOFDM) schemes whose time-domain signal is generated through a direct inverse fast Fourier transform (IFFT), the HACO-OFDM signal is obtained by a superposition of the unipolar time-domain signals of ACO-OFDM and PAM-DMT. Therefore, the conventional PAPR reduction methods are not directly applicable due to their specific superimposed structure. Although the peak power of each of the two signal components can be separately suppressed for example by invoking conventional PAPR reduction for ACO or DMT OFDM, it leads to poor performance because the peak power of HACO-OFDM is not determined by the peak

Manuscript received September 1, 2016; revised February 5, 2017, April 6, 2017, and April 19, 2017; accepted April 23, 2017. Date of publication April 26, 2017; date of current version October 13, 2017. This work was supported in part by the National Basic Research Program of China under Grant 2013CB329204; in part by the European Research Council's Advanced Fellow Grant under the Beam-Me-Up project; in part by the Royal Societys Wolfson Research Merit Award; in part by the NSFC under Grant 61471114, Grant 61571118, and Grant U1534208; in part by the Six talent peaks project in Jiangsu Province under Grant GDZB-005; and in part by the China Scholarship Council. The review of this paper was coordinated by Dr. N.-D. Đào.

B. Li, W. Xu, H. Zhang, and C. Zhao are with the National Mobile Communications Research Laboratory, Southeast University, Nanjing 210096, China (e-mail: martin.libaolong@gmail.com; wxu.seu@gmail.com; huazhang@seu.edu.cn; cmzhao@seu.edu.cn).

L. Hanzo is with the Department of Electronics and Computer Science, University of Southampton, Southampton SO17 1BJ, U.K. (e-mail: lh@ecs.soton.ac.uk).

Color versions of one or more of the figures in this paper are available online at http://ieeexplore.ieee.org.

Digital Object Identifier 10.1109/TVT.2017.2698265

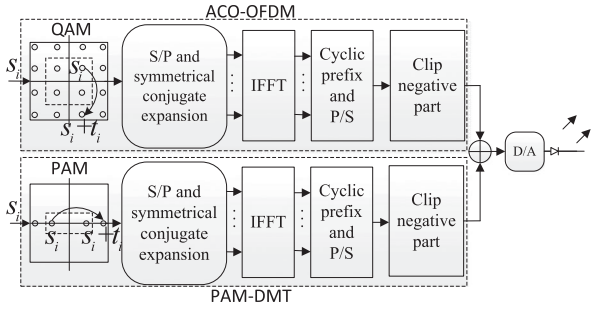

Fig. 1. Transmitter of HACO-OFDM system with tone injection.

power of either ACO-OFDM or PAM-DMT alone, as also evidenced by numerical results.

Against this background, a PAPR reduction method for HACO-OFDM is developed based on the procedure of tone injection, which has been exploited to reduce the PAPR with no bandwidth expansion and a modest increase in bit error ratio (BER) due to the associated average power increase [17], [21]. The main contributions of the paper are summarized as follows.

1) Based on the superimposed feature of the HACO-OFDM, we propose the joint optimization of ACO-OFDM and PAM-MDT tone injection for HACO-OFDM for substantially reducing the PAPR. This is capable of providing a better PAPR reduction performance than separate tone injection applied to both signal components.
2) Due to the nonlinear operation of clipping the negative signal components involved, the original joint tone injection problem of HACO-OFDM becomes intractable. In order to circumvent this problem, we equivalently transform the problem to a tractable linear formulation by exploiting the specific time-domain characteristics of HACO-OFDM signals. Moreover, the transformed problem is equivalent to the original problem, which does not impose any performance degradation.

Then, the transformed linear problem is interpreted as a l_1 minimization problem, which can be efficiently solved. Our numerical results show that the proposed method achieves a lower PAPR than conventional OOFDM schemes.

II. Tone Injection for Hybrid ACO-OFDM

HACO-OFDM improves the spectral efficiency by constructing the modulated signal as a careful superimposition of ACO-OFDM and PAM-DMT signals, as shown in Fig. 1. In ACO-OFDM, the odd subcarriers are quadrature amplitude modulated, while the remaining subcarriers are set to zero. In order to guarantee that the ACO-OFDM symbols are not contaminated by interference, in PAM-DMT only the imaginary part of even subcarriers is modulated by pulse amplitude modulation (PAM) symbols.

Let N be the total number of subcarriers, while $\{s_i\}_{i=0}^{\frac{N}{2}-2}$ the source data of HACO-OFDM, where $s_i = a_i^R + ja_i^I$ $(i = 0, 1, \ldots, N/4-1)$ is a complex-valued QAM symbol, and $s_i = jb_i$ $(i = N/4, \ldots, N/2-2)$ with b_i being a real-valued PAM symbol. The basic idea of tone injection is to exploit the resultant extra degrees of freedom for PAPR reduction through a cyclic extension of the symbol constellation [17]. Letting t_i be the injected tone, after performing tone injection, HACO-OFDM transmits the source data of $\widehat{s}_i = s_i + t_i$, $i = 0, 1, \ldots, N/2-2$. In order to recover the original source data, t_i is set to

$$t_i = \begin{cases} -p_i \mathrm{sgn}(a_i^R) D_i - jq_i \mathrm{sgn}(a_i^I) D_i, & i = 0, \ldots, \dfrac{N}{4} - 1 \\ -jh_i \mathrm{sgn}(b_i) D_i, & i = \dfrac{N}{4}, \ldots, \dfrac{N}{2} - 2. \end{cases} \tag{1}$$

Here, $\mathrm{sgn}(x)$ is the sign of x, D_i is a positive real value chosen for ensuring that $D_i = \rho d_i \sqrt{M_{\mathrm{QAM},i}}$ $(i = 0, \ldots, N/4-1)$ and $D_i = \rho d_i M_{\mathrm{PAM},i}$ $(i = N/4, \cdots N/2-2)$, where d_i denotes the minimum inter-symbol distance, ρ is a real scaling factor, while $M_{\mathrm{QAM},i}$ and $M_{\mathrm{PAM},i}$ are respectively the sizes of the QAM and PAM constellations. In order to avoid reducing the minimum inter-symbol distance of the constellation, ρ should satisfy $\rho \geq 1$ [17]. The injected tone t_i obeying (1) can be removed at the receiver by subjecting the received signals to the modulo-D_i operation. The real scalars p_i, q_i and h_i are the integer decision variables to be optimized. According to [12], it is preferred that

$$\begin{aligned} &p_i \in \{0, 1\}, q_i \in \{0, 1\}, \; i = 0, \ldots, N/4 - 1 \\ &h_i \in \{0, 1\}, \; i = N/4, \ldots, N/2 - 2. \end{aligned} \tag{2}$$

Note that the corresponding subcarrier symbol is shifted, when the decision variable is selected to be 1 and the subcarrier symbol remains unchanged, when the decision variable is 0. At the receiver, we have to subtract the clipping noise imposed on the even subcarriers caused by ACO-OFDM in order to successfully estimate the PAM symbols. In this case, the information concerning the decision variables p_i and q_i for ACO-OFDM is necessary. However, these parameters are not required to be transmitted from the transmitter to the receiver side, since they can be readily estimated by checking whether the received signals of ACO-OFDM fall into the extended area of the constellation.

By assigning $\{\widehat{s}_l\}_{l=0}^{\frac{N}{4}-1}$ and $\{\widehat{s}_m\}_{m=\frac{N}{4}}^{\frac{N}{2}-2}$ to the odd and even subcarriers, as seen Fig. 2, we obtain the frequency-domain signals of ACO-OFDM and PAM-DMT, which are respectively expressed as

$$\widehat{X}_k = \begin{cases} s_l + t_l, & k = 2l + 1 \\ s_l^* + t_l^*, & k = NL - 2l - 1 \\ 0, & \text{otherwise} \end{cases} \tag{3}$$

and

$$\widehat{Y}_k = \begin{cases} s_m + t_m, & k = 2m - \dfrac{N}{2} + 2 \\ s_m^* + t_m^*, & k = NL - 2m + \dfrac{N}{2} - 2 \\ 0, & \text{otherwise} \end{cases} \tag{4}$$

where L is the oversampling factor, $\widehat{X}_k$ and $\widehat{Y}_k$ denote the symbols at the k-th subcarrier of the ACO-OFDM and PAM-DMT, respectively, while the superscript $()^*$ is the conjugate operator. After performing IFFT, the L-times over-sampled time-domain outputs are given by

$$\begin{aligned} \widehat{x}_n &= \frac{1}{\sqrt{NL}} \sum_{k=0}^{NL-1} \widehat{X}_k e^{j2\pi \frac{kn}{NL}} \\ \widehat{y}_n &= \frac{1}{\sqrt{NL}} \sum_{k=0}^{NL-1} \widehat{Y}_k e^{j2\pi \frac{kn}{NL}}, \; n = 0, \ldots, NL-1. \end{aligned} \tag{5}$$

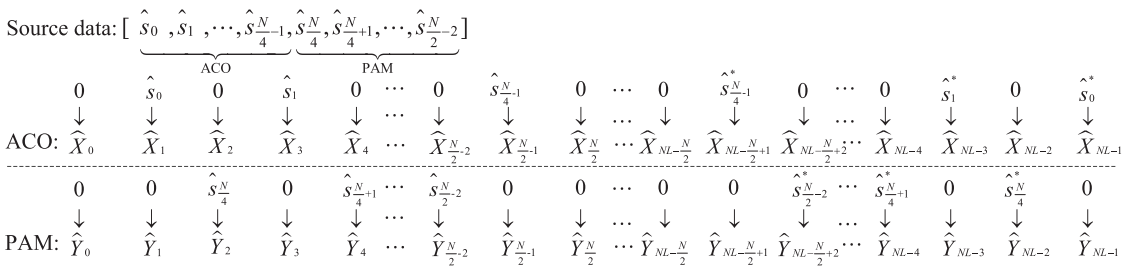

Fig. 2. Frequency-domain symbols of ACO-OFDM and PAM-DMT in HACO-OFDM.

It has been shown that the PAPR computed from the over-sampled signals associated with $L = 2$ or 4 are sufficiently accurate for evaluating the PAPR of a continuous baseband waveform [21]. In contrast to the conventional OOFDM schemes, the time-domain signal of HACO-OFDM is generated by a time-domain superposition of the ACO-OFDM and PAM-DMT signals, which is expressed as

$$\widehat{z}_n = \lfloor \widehat{x}_n \rfloor_c + \lfloor \widehat{y}_n \rfloor_c,\ n = 0, \ldots, NL-1 \tag{6}$$

where $\lfloor x \rfloor_c = \max\{x, 0\}$ represents the nonlinear operation of clipping the negative part of x. The PAPR of HACO-OFDM in (6) is calculated as

$$\text{PAPR} = \frac{\max_{0 \le n \le NL-1} \widehat{z}_n^2}{\text{E}\{\widehat{z}_n^2\}} \tag{7}$$

where $\text{E}\{\cdot\}$ denotes the statistical expectation.

III. Design of Reduced-PAPR HACO-OFDM

In this section, the joint optimization of ACO-OFDM and PAM-DMT tone injection is proposed for HACO-OFDM to mitigate the high PAPR. We first present the non-convex PAPR reduction problem of HACO-OFDM, and then equivalently transform it to a more tractable mixed integer linear programming (MILP) problem by exploiting the time-domain characteristics of HACO-OFDM signals. Finally, the MILP problem is interpreted as a l_1 minimization problem with the aid of the theory of compressed sensing.

A. PAPR Reduction Problem Formulation

We optimize the design of reduced-PAPR HACO-OFDM relying on joint ACO-OFDM and PAM-DMT tone injection, which reduces the peak power of the superimposed signal, i.e. $\max\{[\lfloor \widehat{x}_n \rfloor_c + \lfloor \widehat{y}_n \rfloor_c]^2\}_{n=0}^{NL-1}$, by finding the best choice of the binary integer decision variables. Accordingly, the optimization problem specified for HACO-OFDM can be formulated as

$$\min_{\{p_i, q_i, h_i\}} \max_{0 \le n \le NL-1} \left[\lfloor \widehat{x}_n \rfloor_c + \lfloor \widehat{y}_n \rfloor_c\right]^2,\ \text{s.t.}\,(2). \tag{8}$$

It directly follows from (6) that $\widehat{z}_n = \lfloor \widehat{x}_n \rfloor_c + \lfloor \widehat{y}_n \rfloor_c \ge 0$. Therefore, we can equivalently transform the above optimization problem to

$$\min_{\{p_i, q_i, h_i\}} \max_{0 \le n \le NL-1} \lfloor \widehat{x}_n \rfloor_c + \lfloor \widehat{y}_n \rfloor_c,\ \text{s.t.}\,(2). \tag{9}$$

The objective function of the above problem involves the nonlinear operation of clipping, which makes the problem difficult to address. In order to make the problem tractable, we first analyze the characteristics of HACO-OFDM signals. Then, accordingly, we can simplify the objective in (9) and transform the original problem to a linear programming problem subject to an additional integer constraint.

B. Time-Domain Characteristic Analysis of HACO-OFDM

Let us now focus our attention on the time-domain representation of HACO-OFDM. Based on (6), the legitimate values of $\widehat{z}_n$ can be either of $\widehat{x}_n$, $\widehat{y}_n$, $\widehat{x}_n + \widehat{y}_n$ and 0. Moreover, considering that $\widehat{z}_n = \lfloor \widehat{x}_n \rfloor_c + \lfloor \widehat{y}_n \rfloor_c$, we have

$$\widehat{z}_n \ge \widehat{x}_n,\ \widehat{z}_n \ge \widehat{y}_n,\ \widehat{z}_n \ge \widehat{x}_n + \widehat{y}_n,\ \widehat{z}_n \ge 0\ \forall n. \tag{10}$$

It follows that $\widehat{z}_n = \max\{\widehat{x}_n, \widehat{y}_n, \widehat{x}_n + \widehat{y}_n, 0\}$. Assuming that $\max\{\widehat{z}_n\}_{n=0}^{NL-1} = \widehat{z}_{n^*}$, where n^* is the discrete time corresponding to the maximal time-domain HACO-OFDM signal, we have

$$\begin{aligned} \widehat{z}_{n^*} &= \max\{\widehat{x}_{n^*}, \widehat{y}_{n^*}, \widehat{x}_{n^*} + \widehat{y}_{n^*}, 0\} \\ &= \max_{0 \le n \le NL-1} \{\max\{\widehat{x}_n, \widehat{y}_n, \widehat{x}_n + \widehat{y}_n, 0\}\}. \end{aligned} \tag{11}$$

Furthermore, since it is impossible that '0' is the peak value of HACO-OFDM signals, we have

$$\widehat{z}_{n^*} = \max\{\widehat{x}_{n^*}, \widehat{y}_{n^*}, \widehat{x}_{n^*} + \widehat{y}_{n^*}\}. \tag{12}$$

Observe from (3) and (4) that, as shown in Fig. 2, ACO-OFDM and PAM-DMT occupy only the odd and even subcarriers, respectively. Thus, by exploiting the Hermitian symmetric property of OOFDM, the time-domain signals have to satisfy

$$\widehat{x}_n = -\widehat{x}_{n+\frac{NL}{2}},\ \widehat{y}_n = \widehat{y}_{n+\frac{NL}{2}},\ n = 0, \ldots, NL/2-1. \tag{13}$$

Based on (12) and (13), we infer that if $\widehat{z}_{n^*} = \widehat{y}_{n^*}$ and $n^* < \frac{NL}{2} - 1$, then $\widehat{x}_{n^*} < 0$. The above relationship implies that we have $\widehat{x}_{n^*+\frac{NL}{2}} > 0$ and $\widehat{z}_{n^*+\frac{NL}{2}} = \widehat{x}_{n^*+\frac{NL}{2}} + \widehat{y}_{n^*+\frac{NL}{2}} > \widehat{z}_{n^*}$, which is contradictory to $\max\{\widehat{z}_n\}_{n=0}^{NL-1} = \widehat{z}_{n^*}$. The same conclusion may be inferred for the case of $\widehat{z}_{n^*} = \widehat{y}_{n^*}$ and $n^* > \frac{NL}{2} - 1$. Therefore, it is safe to remove the scenario associated with $\widehat{z}_{n^*} = \widehat{y}_{n^*}$. Then, the relationship in (12) reduces to $\widehat{z}_{n^*} = \max\{\widehat{x}_{n^*}, \widehat{x}_{n^*} + \widehat{y}_{n^*}\}$. Note that $\widehat{x}_{n^*}$ and $\widehat{x}_{n^*} + \widehat{y}_{n^*}$ both belong to the set $\{\widehat{x}_0, \widehat{x}_0 + \widehat{y}_0, \widehat{x}_1, \widehat{x}_1 + \widehat{y}_1, \cdots, \widehat{x}_{NL-1}, \widehat{x}_{NL-1} + \widehat{y}_{NL-1}\}$, which implies that the value of $\widehat{z}_{n^*}$ also belongs to the set. From $\widehat{z}_{n^*} \ge \widehat{z}_n$, we have $\widehat{z}_{n^*} \ge \widehat{x}_n$, $\widehat{z}_{n^*} \ge \widehat{x}_n + \widehat{y}_n\ \forall n$. Therefore, $\widehat{z}_{n^*}$ is the maximum of the set, which is expressed as

$$\widehat{z}_{n^*} = \max\{\widehat{x}_0, \widehat{x}_0 + \widehat{y}_0, \widehat{x}_1, \widehat{x}_1 + \widehat{y}_1, \cdots, \widehat{x}_{NL-1}, \widehat{x}_{NL-1} + \widehat{y}_{NL-1}\}. \tag{14}$$

C. Equivalent Problem Formulation

In this subsection, we will equivalently transform the non-convex PAPR reduction problem in (9) to a more tractable formulation. By

exploiting the equivalence in (14), the optimization problem of (9) can be rewritten as

$$\min_{\{p_i,q_i,h_i\}} \max\{\widehat{x}_0,\widehat{x}_0+\widehat{y}_0,\widehat{x}_1,\widehat{x}_1+\widehat{y}_1,\cdots,\widehat{x}_{NL-1},\widehat{x}_{NL-1}+\widehat{y}_{NL-1}\}$$
$$\text{s.t. } (2). \tag{15}$$

Now, we are ready to transform the problem (15) to a linear program. We commence by introducing a new variable t. Problem (15) is then equivalently transformed to

$$\min_{\{p_i,q_i,h_i\}} \ t$$
$$\text{s.t. } \widehat{x}_n \le t,\ \widehat{x}_n+\widehat{y}_n \le t,\ n=0,\ldots,NL-1$$
$$\text{and } (2). \tag{16}$$

Using (3) and (5), $\widehat{x}_n$ can be expressed as

$$\begin{aligned}\widehat{x}_n &= \frac{1}{\sqrt{NL}}\sum_{l=0}^{N/4-1}\left\{(s_l+t_l)e^{j2\pi\frac{(2l+1)n}{NL}}+(s_l^*+t_l^*)e^{-j2\pi\frac{(2l+1)n}{NL}}\right\}\\ &= \frac{2}{\sqrt{NL}}\sum_{l=0}^{N/4-1}\mathrm{Re}\left\{s_l e^{j2\pi\frac{(2l+1)n}{NL}}\right\}\\ &\quad+\frac{2}{\sqrt{NL}}\sum_{l=0}^{N/4-1}\left\{-p_l\mathrm{sgn}(a_l^R)D_l\cos\left[2\pi n(2l+1)/(NL)\right]\right.\\ &\quad\left.+\ q_l\mathrm{sgn}(a_l^I)D_l\sin\left[2\pi n(2l+1)/(NL)\right]\right\}. \end{aligned}\tag{17}$$

By introducing the following constants:

$$\begin{aligned}x_n &= \frac{2}{\sqrt{NL}}\sum_{l=0}^{N/4-1}\mathrm{Re}\left\{s_l e^{j2\pi\frac{(2l+1)n}{NL}}\right\}\\ \mathbf{c}_n &= \left[c_{n,0},\ldots,c_{n,\frac{N}{4}-1}\right]^T,\ \mathbf{u}_n=\left[u_{n,0},\ldots,u_{n,\frac{N}{4}-1}\right]^T\\ c_{n,l} &= \frac{2}{\sqrt{NL}}\mathrm{sgn}\left(a_l^R\right)D_l\cos\left[2\pi n(2l+1)/(NL)\right]\\ u_{n,l} &= \frac{2}{\sqrt{NL}}\mathrm{sgn}\left(a_l^I\right)D_l\sin\left[2\pi n(2l+1)/(NL)\right]\end{aligned}\tag{18}$$

$\widehat{x}_n$ can be expressed in a compact form as a linear equation:

$$\widehat{x}_n = x_n-\mathbf{p}^T\mathbf{c}_n+\mathbf{q}^T\mathbf{u}_n \tag{19}$$

where $\mathbf{p}=[p_0,\ldots,p_{N/4-1}]^T$ and $\mathbf{q}=[q_0,\ldots,q_{N/4-1}]^T$ are the optimization vectors. Similarly, $\widehat{y}_n$ can be rewritten as

$$\widehat{y}_n = y_n+\mathbf{h}^T\mathbf{w}_n \tag{20}$$

where $\mathbf{h}=[h_{N/4},\ldots,h_{N/2-2}]^T$ is the optimization vector and the constants y_n and $\mathbf{w}_n$ are defined as

$$\begin{aligned}y_n &= \frac{2}{\sqrt{NL}}\sum_{m=N/4}^{N/2-2}\mathrm{Re}\left\{s_m e^{j\pi\frac{(4m-N+4)n}{NL}}\right\}\\ \mathbf{w}_n &= \left[w_{n,\frac{N}{4}},\ldots,w_{n,\frac{N}{2}-2}\right]^T\\ w_{n,m} &= \frac{2}{\sqrt{NL}}\mathrm{sgn}(b_m)D_m\sin\left[\pi n\frac{4m-N+4}{NL}\right].\end{aligned}\tag{21}$$

Thus, the optimization problem of (16) can be rewritten as

$$\min_{\mathbf{p},\mathbf{q},\mathbf{h},t}\ t$$
$$\text{s.t. } x_n+y_n-\mathbf{p}^T\mathbf{c}_n+\mathbf{q}^T\mathbf{u}_n+\mathbf{h}^T\mathbf{w}_n\le t$$
$$x_n-\mathbf{p}^T\mathbf{c}_n+\mathbf{q}^T\mathbf{u}_n\le t,\ n=0,\cdots NL-1$$
$$\mathbf{p}\in\{0,1\}^{\frac{N}{4}},\mathbf{q}\in\{0,1\}^{\frac{N}{4}},\mathbf{h}\in\{0,1\}^{\frac{N}{4}-1} \tag{22}$$

where $\{0,1\}^m$ represents the set of m-dimensional binary vectors. By stacking all variables as a new vector $\mathbf{v}=[\mathbf{p}^T,\mathbf{q}^T,\mathbf{h}^T]^T$, we can further rewrite (22) as

$$\min_{\mathbf{v},t}\ t,\ \text{s.t. } \mathbf{z}+\mathbf{A}\mathbf{v}\le t\mathbf{1}_{2NL},\ \mathbf{v}\in\{0,1\}^{\frac{3N}{4}-1} \tag{23}$$

where $\mathbf{1}_m$ represents the all-one vector of size m, while $\mathbf{z}$ and $\mathbf{A}$ are constants defined as

$$\begin{aligned}\mathbf{z} &= [x_0,\ldots,x_{NL-1},x_0+y_0,\ldots,x_{NL-1}+y_{NL-1}]^T\\ \mathbf{A} &= \begin{bmatrix}-\mathbf{C} & \mathbf{U} & \mathbf{0}_{NL\times(\frac{N}{4}-1)}\\ -\mathbf{C} & \mathbf{U} & \mathbf{W}\end{bmatrix}\\ \mathbf{C} &= [\mathbf{c}_0,\ldots,\mathbf{c}_{NL-1}]^T,\mathbf{U}=[\mathbf{u}_0,\cdots,\mathbf{u}_{NL-1}]^T\\ \mathbf{W} &= [\mathbf{w}_0,\ldots,\mathbf{w}_{NL-1}]^T.\end{aligned}\tag{24}$$

Clearly, the problem in (23) is a well-structured linear problem with binary integer constraints, which is a MILP problem [22]. The MILP can be solved by the state-of-the-art software, such as CPLEX [23]. However, in the specific problem encountered here, we will invoke the compressed sensing techniques to solve the problem more efficiently.

D. Compressed-Sensing-Based Solution

In this subsection, enlightened by the pioneering work in [24], we resort to the theory of compressed sensing to relax the integer constraints in (23). It has been observed in [17], [21], and [24] that the tone injection scheme only needs a few subcarrier symbol shifts to achieve a low PAPR. Therefore, the problem in (23) has a sparse solution concerning $\mathbf{v}$. Based on the theory of compressed sensing [25], we can solve the problem in (23) with the aid of a sparse solution $\mathbf{v}$ by opting for solving the following l_1-minimization problem:

$$\min_{\mathbf{v}}\ \|\mathbf{v}\|_1$$
$$\text{s.t. } \mathbf{z}+\mathbf{A}\mathbf{v}\le t_T\mathbf{1}_{2NL},\ \mathbf{0}_{\frac{3N}{4}-1}\le\mathbf{v}\le\mathbf{1}_{\frac{3N}{4}-1} \tag{25}$$

where $\|\cdot\|_1$ denotes the l_1-norm of the vector, and t_T denotes the target maximum of $\widehat{z}_n$. The powerful l_1-minimization belongs to the class of compressed sensing problems, which can be efficiently solved by diverse mature methods, such as the simplex algorithm of [22]. Note that the solution of (25), denoted by $\mathbf{v}^*=[v_0^*,\ldots,v_{3N/4-1}^*]^T$, does not in general assume integer values. Since $v_k^*\in[0,1]$, we interpret v_k^* as the probability of shifting the corresponding subcarrier symbol. Then, we randomly generate multiple tone injection candidate solutions associated with the probability $\mathbf{v}^*$ and then select the one that achieves the lowest PAPR as the desired solution.

Next, we will analyze the influence of the number of tone injection candidate solutions on the complexity. Let $\widehat{\mathbf{v}}_k$ and N_c represent the

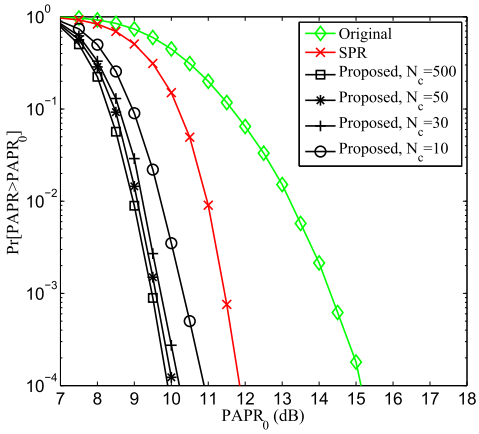

Fig. 3. CCDF curves of the PAPR for 16-HACO-OFDM.

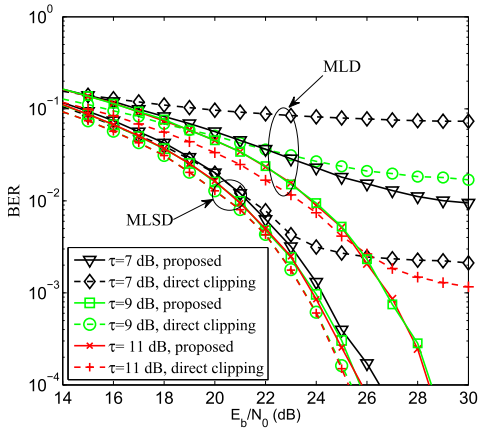

Fig. 4. BER comparison of the 16-HACO-OFDM systems using the proposed method and direct clipping.

kth candidate solution and the number of candidates, respectively. The time-domain HACO-OFDM signal corresponding to the kth candidate solution is given by $\widehat{\mathbf{z}}_k = \mathbf{z} + \mathbf{A}\widehat{\mathbf{v}}_k$, $k = 1, \ldots, N_c$. Then, the desired candidate solution is chosen by finding the minimum one in the set $\{||\widehat{\mathbf{z}}_k||_0\}_{k=1}^{k=N_c}$, where $||\cdot||_0$ denotes the l_0 norm of a vector. Since $\mathbf{v}^*$ is sparse and $\widehat{\mathbf{v}}_k$ is generated according to $\widehat{\mathbf{v}}^*$, most of the elements in $\widehat{\mathbf{v}}_k$ is equal to zero, while the rest of the elements are equal to one. Therefore, only a few additions are involved during calculating $\widehat{\mathbf{z}}_k$. The complexity is mainly determined by finding the desired candidate solution, i.e., by finding the minimum and maximum in an unsorted array of size $N_c NL$. Clearly, this has a computational complexity on the order of $O(N_c NL)$.

IV. Numerical Results

The performance of the proposed reduced-PAPR HACO-OFDM is investigated in this section. In our simulation, we consider HACO-OFDM systems associated with $N = 64$ subcarriers, and an over-sampling factor of $L = 2$. Like in [8], an equal proportion of power is allocated to both PAM-DMT and ACO-OFDM. Since HACO-OFDM uses a combination of ACO-OFDM and PAM-DMT, again, a direct PAPR reduction method conceived for HACO-OFDM is to reduce the PAPR of ACO-OFDM and PAM-DMT separately using existing methods [17]. Therefore, we also present the performance of separate PAPR reduction (SPR) of ACO-OFDM and PAM-DMT using the methods of [17] for comparison.

Fig. 3 portrays the complimentary cumulative distribution function (CCDF) curves of the PAPR for 16-HACO-OFDM, namely ACO-OFDM-16QAM associated with PAM-DMT-16PAM. Observe from the figure that a significant PAPR reduction is obtained in the CCDF curve by the proposed method, hence substantially relaxing the linearity requirement of the optical front end. Additionally, the SPR method exhibits a much higher PAPR than the proposed reduced-PAPR HACO-OFDM, because the HACO-OFDM signal is jointly optimized. It is also observed from the figure that a further PAPR reduction can be achieved for larger number of candidate solutions. The tone injection method associated with $N_c = 50$ results in a modest PAPR performance loss compared to the case of $N_c = 500$. Therefore, we opt for the number of candidates to be $N_c = 50$ in the following simulations.

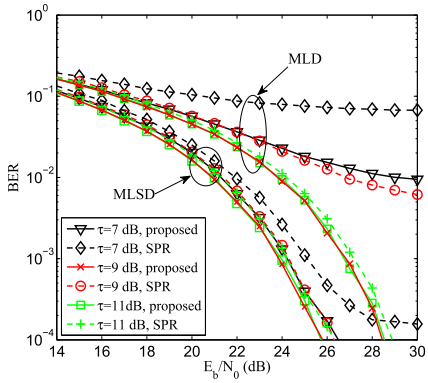

Fig. 5. BER comparison of the 16-HACO-OFDM systems using the proposed method and the SPR method.

Moreover, we investigate the BER performance of the proposed reduced-PAPR HACO-OFDM relying on a realistic nonlinear optical front end, which relies on double-sided amplitude clipping of the analog baseband signals [17]

$$x_{\text{clip}}(t) = \begin{cases} A, & x(t) \geq A \\ x(t), & 0 \leq x(t) < A \\ 0, & x(t) < 0. \end{cases} \tag{26}$$

The clipping ratio is defined as $\tau = 20\log_{10}(A/\sigma)$, where σ^2 is the power of $x(t)$. A low PAPR is capable of reducing the nonlinear distortion of the signals and thus leads to an improved BER performance.

In Fig. 4, we present the BER of the 16-HACO-OFDM systems using the proposed method and direct clipping at different electrical bit energy to noise power ratio E_b/N_0 in conjunction with $\tau = 7$, 9, 13 dB. Both the conventional maximum likelihood detection (MLD) and the low-complexity near-optimal maximum likelihood sequence detection (MLSD) from [26] are employed to detect the transmitted symbols. It is clearly observed that at the relatively low clipping levels, the proposed HACO-OFDM suffers from aw slight BER performance loss due to the average power increase caused by the injected tone. However, for high clipping levels, say at $\tau = 7$ dB, the proposed HACO-OFDM system

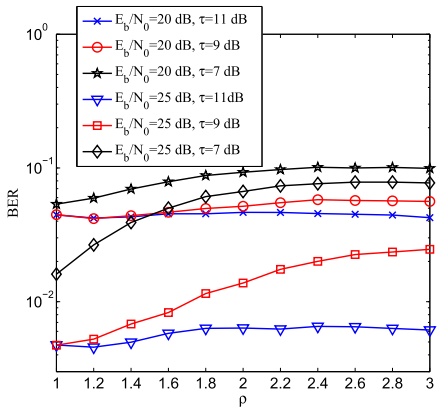

Fig. 6. BER of the proposed 16-HACO-OFDM system at different values of ρ.

enjoys a significant BER performance improvement, thanks to its lower PAPR. Fig. 5 portrays the BER curves of the 16-HACO-OFDM systems using the proposed method and SPR method, where we can observe that the proposed HACO-OFDM system performs noticeably better than the SPR method in terms of the BER.

Next, we will discuss the influence of D_i on the BER performance. The BER performance of the proposed 16-HACO-OFDM system at different values of ρ is presented in Fig. 6. We can observe that a better BER performance can be achieved when the value of ρ is close to one. Moreover, for a high clipping level of $\tau = 7$ dB, the BER performance significantly degrades upon increasing τ, implying that a small ρ increases the resistance to nonlinearity.

V. Conclusion

We developed a specific PAPR reduction technique for HACO-OFDM based on the characteristics of HACO-OFDM signals and by exploiting compressed sensing. Our results have shown that the proposed HACO-OFDM scheme is capable of achieving a much lower PAPR than conventional methods. In the presence of realistic nonlinear optical front-ends, a significant BER performance gain is observed for the proposed HACO-OFDM scheme.

References

[1] D. Tsonev *et al.*, "A 3-Gb/s single-LED OFDM-based wireless VLC link using a gallium nitride LED," *IEEE Photon. Technol. Lett.*, vol. 26, no. 7, pp. 637–640, Apr. 2014.
[2] J. M. Kahn and J. R. Barry, "Wireless infrared communications," *Proc. IEEE*, vol. 85, no. 2, pp. 265–298, Feb. 1997.
[3] J. Jiang, R. Zhang, and L. Hanzo, "Analysis and design of three-stage concatenated color-shift keying," *IEEE Trans. Veh. Technol.*, vol. 64, no. 11, pp. 5126–5136, Nov. 2015.
[4] J. B. Carruthers and J. M. Kahn, "Multiple-subcarrier modulation for nondirected wireless infrared communication," *IEEE J. Sel. Areas Commun.*, vol. 14, no. 3, pp. 538–546, Apr. 1996.
[5] S. Dimitrov, S. Sinanovic, and H. Haas, "Clipping noise in OFDM-based optical wireless communication systems," *IEEE Trans. Commun.*, vol. 60, no. 4, pp. 1072–1081, Apr. 2012.
[6] J. Armstrong and A. J. Lowery, "Power efficient optical OFDM," *Electron. Lett.*, vol. 42, no. 6, pp. 370–372, Mar. 2006.
[7] S. Lee, S. Randel, F. Breyer, and A. Koonen, "PAM-DMT for intensity-modulated and direct-detection optical communication systems," *IEEE Photon. J.*, vol. 21, no. 23, pp. 1749–1751, Dec. 2009.
[8] B. Ranjha and M. Kavehrad, "Hybrid asymmetrically clipped OFDM-based IM/DD optical wireless system," *J. Opt. Commun. Netw.*, vol. 6, no. 4, pp. 387–396, Apr. 2014.
[9] Q. Wang, Z. Wang, and L. Dai, "Iterative receiver for hybrid asymmetrically clipped optical OFDM," *J. Lightw. Technol.*, vol. 32, no. 22, pp. 4471–4477, Nov. 2014.
[10] H. Elgala, R. Mesleh, and H. Haas, "A study of LED nonlinearity effects on optical wireless transmission using OFDM," in *Proc. Wireless Opt. Commun. Netw.*, Apr. 2009, pp. 1–5.
[11] J. Armstrong, "OFDM for optical communications," *J. Lightw. Technol.*, vol. 27, no. 3, pp. 189–204, Feb. 2009.
[12] W. Wang, M. Hu, Y. Li, and H. Zhang, "A low-complexity tone injection scheme based on distortion signals for PAPR reduction in OFDM systems," *IEEE Trans. Broadcast.*, vol. 62, no. 4, pp. 948–956, Dec. 2016.
[13] Z. Yu, "Optical wireless communications with optical power and dynamic range constrains," Ph.D. dissertation, Dept. Elect. Comput. Eng., Georgia Inst. Tech., Atlanta, GA, USA, May 2014.
[14] S. Dimitrov and H. Haas, "Information rate of OFDM-based optical wireless communication systems with nonlinear distortion," *J. Lightw. Technol.*, vol. 31, no. 6, pp. 918–929, Mar. 2013.
[15] W. Xu, M. Wu, H. Zhang, X. You, and C. Zhao, "ACO-OFDM-specified recoverable upper clipping with efficient detection for optical wireless communications," *IEEE Photon. J.*, vol. 6, no. 5, pp. 1–17, Oct. 2014.
[16] H. Chen, J. He, J. Tang, F. Li, M. Chen, and L. Chen, "Performance of 16 QAM-OFDM with new null subcarrier shifting in an intensity-modulated direct detection system," *J. Opt. Commun. Netw.*, vol. 6, no. 2, pp. 159–164, Feb. 2014.
[17] H. Zhang, Y. Yuan, and W. Xu, "PAPR reduction for DCO-OFDM visible light communications via semidefinite relaxation," *IEEE Photon. Technol. Lett.*, vol. 26, no. 17, pp. 1718–1721, Sep. 2014.
[18] W. Popoola, Z. Ghassemlooy, and B. Stewart, "Pilot-assisted PAPR reduction technique for optical OFDM communication systems," *J. Lightw. Technol.*, vol. 32, no. 7, pp. 1374–1382, Apr. 2014.
[19] F. Ogunkoya, W. Popoola, A. Shahrabi, and S. Sinanovic, "Performance evaluation of pilot-assisted PAPR reduction technique in optical OFDM systems," *IEEE Photon. Technol. Lett.*, vol. 27, no. 10, pp. 1088–1091, May 2015.
[20] J. Zhou and Y. Qiao, "Low-PAPR asymmetrically clipped optical OFDM for intensity-modulation/direct-detection systems," *IEEE Photon. J.*, vol. 7, no. 3, pp. 1–8, Jun. 2015.
[21] N. Jacklin and Z. Ding, "A convex optimization approach to reducing peak-to-average-power ratio in OFDM," in *Proc. IEEE Int. Symp. Circuits Syst.*, May 2011, pp. 973–976.
[22] G. Sierksma, *Linear and Integer Programming: Theory and Practice, Second Edition*. Boca Raton, FL, USA: CRC, 2001.
[23] M. Carrión and J. M. Arroyo, "A computationally efficient mixed-integer linear formulation for the thermal unit commitment problem," *IEEE Trans. Power Syst.*, vol. 21, no. 3, pp. 233–236, Aug. 2006.
[24] N. Jacklin and Z. Ding, "A linear programming based tone injection algorithm for PAPR reduction of OFDM and linearly precoded systems," *IEEE Trans. Circuits Syst.*, vol. 60, no. 7, pp. 1937–1945, Jul. 2013.
[25] D. Donoho, "Compressed sensing," *IEEE Trans. Inf. Theory*, vol. 52, no. 4, pp. 1289–1306, Apr. 2006.
[26] J. Tan, Z. Wang, Q. Wang, and L. Dai, "Near-optimal low-complexity sequence detection for clipped DCO-OFDM," *IEEE Photon. Technol. Lett.*, vol. 28, no. 3, pp. 233–236, Feb. 2016.